Can Radio Emission Escape from the Magnetosphere of υ andromedae b - a new method to constrain the minimum mass of hot jupiters

N. V. Erkaev, C. Weber, Jean-Mathias Griessmeier, H. Lammer, V. A. Ivanov, P. Odert

Monthly Notices of the ROYAL ASTRONOMICAL SOCIETY

MNRAS **512,** 4869–4876 (2022) https://doi.org/10.1093/mnras/stac767
Advance Access publication 2022 March 21

Can radio emission escape from the magnetosphere of υ Andromedae b – a new method to constrain the minimum mass of Hot Jupiters

N. V. Erkaev,[1,2,3]★ C. Weber,[4] J.-M. Grießmeier,[5,6]★ H. Lammer,[4] V. A. Ivanov[1,3] and P. Odert[7]

[1]*The Applied Mechanics Department, Siberian Federal University, 660074 Krasnoyarsk, Russian Federation*
[2]*Institute of Computational Modelling, Siberian Branch of the Russian Academy of Sciences, 660036 Krasnoyarsk, Russian Federation*
[3]*Institute of Laser Physics, Siberian Branch of the Russian Academy of Sciences, 630090 Novosibirsk, Russian Federation*
[4]*Space Research Institute, Austrian Academy of Sciences, Schmiedlstr 6, A-8042 Graz, Austria*
[5]*LPC2E - Université d'Orléans / CNRS, F-45071 Orléans cedex 2, France*
[6]*Station de Radioastronomie de Nançay, Observatoire de Paris, PSL Research University, CNRS, Univ. Orléans, OSUC, F-18330 Nançay, France*
[7]*Institute of Physics/IGAM, University of Graz, Universitätsplatz 5, A-8010 Graz, Austria*

Accepted 2022 March 16. Received 2022 March 16; in original form 2021 November 12

ABSTRACT

We investigate the atmospheric and magnetospheric conditions of the massive, close-in exoplanet υ Andromedae b (hereafter ups And b). In particular, we explore whether radio emission can be produced by the Cyclotron Maser Instability (CMI), and whether this emission can escape from its source region. For this, we compare the local cyclotron frequency to the local plasma frequency. The planetary mass has a decisive impact on both of these frequencies: the cyclotron frequency depends on the (mass-dependent) estimate of the planetary magnetic moment, and the plasma frequency is determined by the (gravity-dependent) atmospheric profile. For this reason, the planetary mass is one of the decisive parameters determining whether the CMI can operate efficiently. As the precise planetary mass is unknown in the case of ups And b, we compare the plasma conditions for a range of hypothetical masses of the planet in order to determine at which mass the atmosphere becomes 'compact', i.e. is not strongly extended, and thus provides favourable conditions for the CMI. In the case of detected planetary radio emission, this approach can provide a new way to constrain the mass of an exoplanet for which only a minimum mass is known.

Key words: planets and satellites: atmospheres – planets and satellites: aurorae – planets and satellites: detection – planets and satellites: magnetic fields – planet–star interactions – radio continuum: planetary systems.

1 INTRODUCTION

It is known that the Solar system planets emit low-frequency, coherent, polarized radio emission via the so-called Cyclotron Maser Instability (CMI). This instability is based on electric fields parallel to the magnetic field, which accelerate electrons towards the planet into a region of increasing magnetic field (e.g. Zarka 1998; Farrell, Desch & Zarka 1999; Ergun et al. 2000; Treumann 2006). The electrons are partially reflected upwards and some are lost to the planetary atmosphere. The reflected electrons exhibit an unstable distribution, e.g. a loss cone or a horseshoe distribution (e.g. Ergun et al. 2000). For the CMI to operate, the local electron plasma frequency has to be smaller than the local electron cyclotron frequency by a certain factor. Theoretical work suggests a critical ratio, such that the condition for CMI emission becomes $f_p/f_c < 0.4$ (e.g. Le Queau, Pellat & Roux 1985; Hilgers 1992; Zarka, Queinnec & Crary 2001), where f_p and f_c are the plasma and cyclotron frequency, respectively. Both quantities are defined in Section 3. Thus, the CMI requires regions of low plasma density and strong magnetic field.

Once a radio wave is generated at an altitude R_0 with a frequency $f_{wave} = f_c(R_0)$, it can escape from the planetary environment to space if $f_p(r) < f_c(R_0)$ for all distances $r > R_0$. Especially for Hot Jupiters, there can be situations where the upper atmosphere is heated by the high X-ray and EUV (XUV) flux of the host star, which results in expanded upper atmospheres where the ionized gas can prevent the generation and/or escape of radio emission. This effect has already been demonstrated by analytical calculations (Weber et al. 2017a, b, 2018) as well as by numerical simulations (Daley-Yates & Stevens 2017, 2018).

The details of this quenching of the radio emission do, however, depend on the planet. For example, the ratio f_p/f_c varies as a function of altitude, and thus depends on the atmospheric stratification. Models of the planetary magnetosphere can be combined with upper atmosphere models to evaluate whether a given planet is expected to be a potential source of planetary radio emission. Among the most critical parameters are the planetary magnetic field, the planetary orbital distance, and XUV-heating and expansion of the upper atmosphere as well as the planetary mass. Previous studies (e.g. Weber et al. 2017a, b, 2018) have shown that a 'compact' atmosphere can lead to favourable conditions for the generation and escape of radio waves. On the other hand, a strongly 'extended' and ionized upper atmosphere has unfavourable conditions, and will lead to quenching of the planetary radio emission. Weber et al. (2017a, b) found that Hot Jupiters with a relatively low mass, such as HD 209458b ($M < M_J$, where $M_J = 1.898 \times 10^{27}$ kg is the mass of Jupiter), have extended and heated upper atmospheres and upward flowing ionospheres, which makes it hard or even impossible for

★ E-mail: nerkaev@gmail.com (NVE); jean-mathias.griessmeier@cnrs-orleans.fr (J-MG)

generated radio waves to escape from the source region. Similarly, quenching is expected to occur for HD 189733b (Weber et al. 2017b). For the more massive planet τ Bootis b (hereafter tau Boo b, $M > 4M_J$), the atmosphere is 'compact'; in this case, radio emission is not only expected to be generated, but also to easily escape (Weber et al. 2018).

In this work, we apply the approach that was previously used by Weber et al. (2018) for the extrasolar planet tau Boo b to υ Andromedae b (hereafter ups And b) to study whether the planet is a likely source of detectable radio emission. This interest is motivated by the recent findings of Turner et al. (2021), who reported on radio observations of three exoplanetary systems using the Low Frequency Array (LOFAR), namely tau Boo, ups And, and 55 Cnc. For the tau Boo system, Turner et al. (2021) tentatively detect circularly polarized bursty emission in the range 14–21 MHz, with a statistical significance of $\sim 3\sigma$. This discovery agrees with the hypotheses published by Weber et al. (2018), that tau Boo b is a very good candidate for radio emissions produced by the CMI. The authors found that the planet tau Boo b is massive enough to host a 'compact' atmosphere, despite its close-in orbit. They came to the conclusion that radio emission could potentially be generated and escape, which is compatible with the observation of Turner et al. (2021). For the ups And system, Turner et al. (2021) report one LOFAR observation with a $\sim 2\sigma$ marginal signal for bursty emission in the frequency range of 14–38 MHz. In both cases (tau Boo b and ups And b), a planetary origin for the radio signal is the most likely scenario, but a stellar origin cannot be completely ruled out. If confirmed, these detections may constitute the first discovery of exoplanetary radio emission.

For the planet ups And b, CMI quenching has not yet been studied. Indeed, this planet poses the additional problem that the true planetary mass is currently unknown. From radial velocity measurements, we only know the minimum mass. In this study, we treat the planetary mass as a free parameter and investigate CMI quenching for the planet ups And b for various mass cases. We determine the critical mass above which the planetary atmosphere and its related plasma environment can be considered as 'compact' due to gravitational contraction, allowing the CMI to operate.

We also discuss how the study of CMI quenching can serve as a new way to constrain the masses of exoplanets for cases in which only the minimum mass is known from radial velocity observations and is not large enough for providing favourable conditions for the CMI to operate. Combined with radio detections of exoplanets, this can allow to establish a higher minimum value for the planetary mass than the value obtained from radial velocity observations.

This article is structured as follows: In Section 2, we describe the used planetary and stellar parameters and give a brief description of the model. In Section 3, we describe the planetary plasma environment. Section 4 discusses the possibility of generation and escape of radio emission as a function of the mass of the planet ups And b, and Section 5 contains concluding remarks.

2 PARAMETERS AND APPLIED MODEL

Upsilon Andromedae is a binary star system which consists of an F-type main-sequence star ups And A and a smaller M-type star. The innermost planet orbiting ups And A, ups And b, was discovered by the radial velocity method during 1996 by Butler et al. (1997). However, after the discovery of ups And b, there still remained significant residuals in the radial velocity measurements, so that it was found that a three-planet model fits the data best (Butler et al. 1999). In the meantime a fourth Jupiter-like exoplanet was discovered (Curiel et al. 2011; Deitrick et al. 2015). Because of these discoveries ups And A was the first multiple-planetary system that was observed around a main-sequence star and hence the first multiple-planetary system known in a multiple-star system (Roell et al. 2012).

Ryabov, Zarka & Ryabov (2004), Winterhalter et al. (2006), and Shiratori et al. (2006) tried to observe radio emission from ups And b, without any detection. As mentioned before, Turner et al. (2021) reported a radio observation from ups And b using LOFAR. For investigating under which conditions and planetary parameters a CMI-like process should work on this particular planet we use the parameters for ups And b and its host star that are shown in Table 1. Some of these values are further discussed in the following subsections, as noted in the third column of the table.

Table 1. Parameters of ups And b and of its host star. The stellar and planetary parameters are from http://exoplanet.eu/catalog/ups_and_b/, accessed on 2021 September 13. υ_{sw} and n_{sw} are the stellar wind velocity and density, respectively. Some key parameters are further discussed in different sections, as indicated in column 3.

Planet	ups And b	Section
Orbital distance	0.059 au	
Minimum mass	$> 0.62\ M_J$	Section 2.1
Radius	unknown (we assume 1 R_J)	Section 2.1
Dipole moment $\mathcal{M}$	depends on planetary mass	Section 2.2
υ_{sw} at orbit	270 km s^{-1}	Section 2.2
n_{sw} at orbit	4.16×10^{10} m^{-3}	Section 2.2
Atmospheric temperature T_0	2000 K	Section 2.3
Atmospheric pressure P_0	0.1 bar	Section 2.3
XUV flux at orbit	5.4564 Jm^{-2} s^{-1}	Section 2.3
Star	ups And	Ref.
Spectral type	F8 V [(a)]	
Mass	$1.27\ M^a_{Sun}$	
Radius	$1.631\ R^b_{Sun}$	
Age	3.8 Gyr[a]	
Distance	13.47 pc[a]	

Notes. [a]Fuhrmann, Pfeiffer & Bernkopf (1998).
[b]Baines et al. (2008).

2.1 Planetary mass and radius

The true mass of the planet ups And b is currently unknown. From radial velocity measurements, one only knows the minimum mass, $M_{obs} = 0.62\ M_J$ (Ligi et al. 2012). For geometrical reasons, the planetary mass is likely to be close to, but slightly higher than, this minimum mass. For example, the median mass is given by $M_{median} = M_{obs} \cdot \text{median}\left(\frac{1}{\sin i}\right) = \sqrt{4/3}\ M_{obs} \approx 1.15\ M_{obs}$ (Grießmeier, Zarka & Spreeuw 2007). Without extra knowledge, this would mean the median mass of ups And b is 0.71 M_J. By definition, there would be a probability of 50 per cent that the real mass of ups And b is between $M_{obs} = 0.62\ M_J$ and $M_{median} = 0.71\ M_J$. However, this is only true if no additional information is available. For the ups And system, additional constraints are provided by planets c and d of the system. Ito & Miyama (2001) inferred a maximum mass by constraining sin$i$ using stability calculations. Indeed, the gravitational interaction between the planets of the system is stronger for higher planetary masses, allowing the calculation of a maximum planetary mass before the system becomes unstable. Assuming coplanarity between the planets b, c, and d, they find that the mass of ups And b is at most 1.43 times the minimum mass obtained from radio velocity observations, i.e. 0.9 M_J. McArthur et al. (2010) recalculated the potential stability of the system without the

Table 2. Exobase distance and magnetic moments for the different mass cases studied in Section 2.3. Column 1: planetary mass. Column 2: exobase distance (in planetary radii). Column 3: expected magnetic moment (under the hypothesis that planetary rotation does not have any influence on the planetary magnetic field). Column 4: expected magnetic moment (under the hypothesis that planetary rotation has a strong influence on the planetary magnetic field, and the planet is tidally locked). Column 5: expected standoff distance with the magnetic field of column 3. Column 6: expected standoff distance with the magnetic field of column 4.

Planetary mass [M_J]	Exobase distance [R_p]	Magnetic moment (no rot effect) [$\mathcal{M}_J$]	Magnetic moment (rot effect) [$\mathcal{M}_J$]	Standoff distance (no rot effect) [R_p]	Standoff distance (rot effect) [R_p]
0.62	3.4	0.60	0.1	6.7	3.7
0.8	3.0	0.80	0.13	7.4	4.0
1.0	2.6	1.00	0.16	7.9	4.3
1.25	1.9	1.21	0.20	8.5	4.6
1.5	1.5	1.44	0.23	9.0	4.9
2.0	1.3	1.73	0.28	9.5	5.2
2.25	1.26	1.87	0.30	9.8	5.3
2.5	1.22	2.00	0.32	10.0	5.4
3.0	1.17	2.25	0.36	10.4	5.6

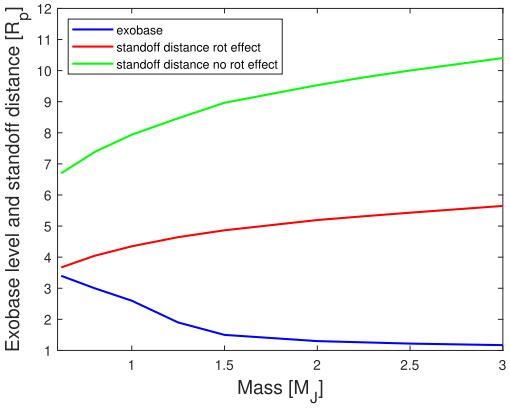

Figure 1. Exobase distance and standoff distance (in planetary radii) as a function of the planetary mass.

assumption of coplanarity, and added new observational constraints. From astrometric observations, they find that the outer planets (c and d) have true masses that are higher than their radial-velocity-derived minimum masses; it seems likely that the inclination of the orbit of planet b is also far from 90°. Following a stability analysis, McArthur et al. (2010) concluded that the mass of ups And b is likely 1–2 M_J, with a median value across their stable realizations at 1.7 M_J. In the following text, we treat the planetary mass as a free parameter. We investigate the range between $M_{\min} = 0.62\,M_J$ and $M = 3\,M_J$.

As the planet is not transiting its star, its radius is also unknown. We assume a planetary radius of $R_p = 1\,R_J$, where $R_J = 7.1492 \times 10^7$m is the radius of Jupiter (see Table 1). For a cold gaseous giant with a mass of 0.62 M_J or more, typical mass–radius relationships (e.g. Grießmeier et al. 2007, Appendix A.2) give values between 0.93 and 1.16 R_J (the latter being the maximum radius). Knowing that Hot Jupiters have an increased radius when compared to a cold planet, a lower limit of 1.0 R_J is assumed. We have checked that an increase of the assumed planetary radius R_p by up to 20 per cent, i.e. up to 1.2 R_J, does not change our results qualitatively.

2.2 Planetary magnetic field

One of the important parameters which determines whether radio emission is generated and can escape to space is the planetary magnetic field. In the following text, we try to estimate this parameter.

For this, we use similar assumptions as previous studies (Grießmeier et al. 2007; Grießmeier, Zarka & Girard 2011; Griessmeier 2017). In particular, we compare two different hypotheses concerning the planetary magnetic field:

(i) We first assume that the planetary magnetic field is independent of planetary rotation (as was suggested e.g. by Reiners & Christensen 2010, although we do not take their age-dependence of the planetary magnetic moment into account). Note that the same result is obtained for planets that are far from their host star and are not affected by tidal locking.

(ii) We then assume that the low rotation rate induced by tidal locking of close-in planets leads to a smaller planetary magnetic field (as suggested e.g. by Grießmeier et al. 2004; Griessmeier 2017).

Table 2 shows the magnetic moments for each (hypothetical) planetary mass case for both magnetic field models. For this, we normalize to Jupiter's magnetic moment, using $\mathcal{M}_J = 1.56 \times 10^{27}$ Am^2. Without any surprise, more massive planets are expected to host a larger magnetic field. Also, the magnetic field values are much lower if tidal locking is assumed to have an influence on the magnetic field ('rot effect' model) than if the magnetic field is assumed to be independent of the planetary rotation ('no rot effect' model). For the cases considered in this work, tidal locking leads to a decrease of the planetary magnetic field by a factor of ∼6.

The planetary magnetic moment has two consequences which are of relevance to this study. First, it determines the standoff distance, i.e. the distance at which the magnetic pressure of the planetary magnetic field balances the ram pressure of the stellar wind (calculated in the same way as Weber et al. 2018). The resulting values are given in Table 2 and also shown in Fig. 1.

Second, the planetary magnetic moment can also be used to estimate the maximum emission frequency and the flux density of planetary radio emission. For ups And b, Reiners & Christensen (2010) predict a dipole magnetic field strength at the pole of 10 G, corresponding to a magnetic moment similar to that of Jupiter. From this, they obtain a radio flux of 41.8 mJy and a maximum emission frequency of 27 MHz. By contrast, Grießmeier et al. (2011) find a

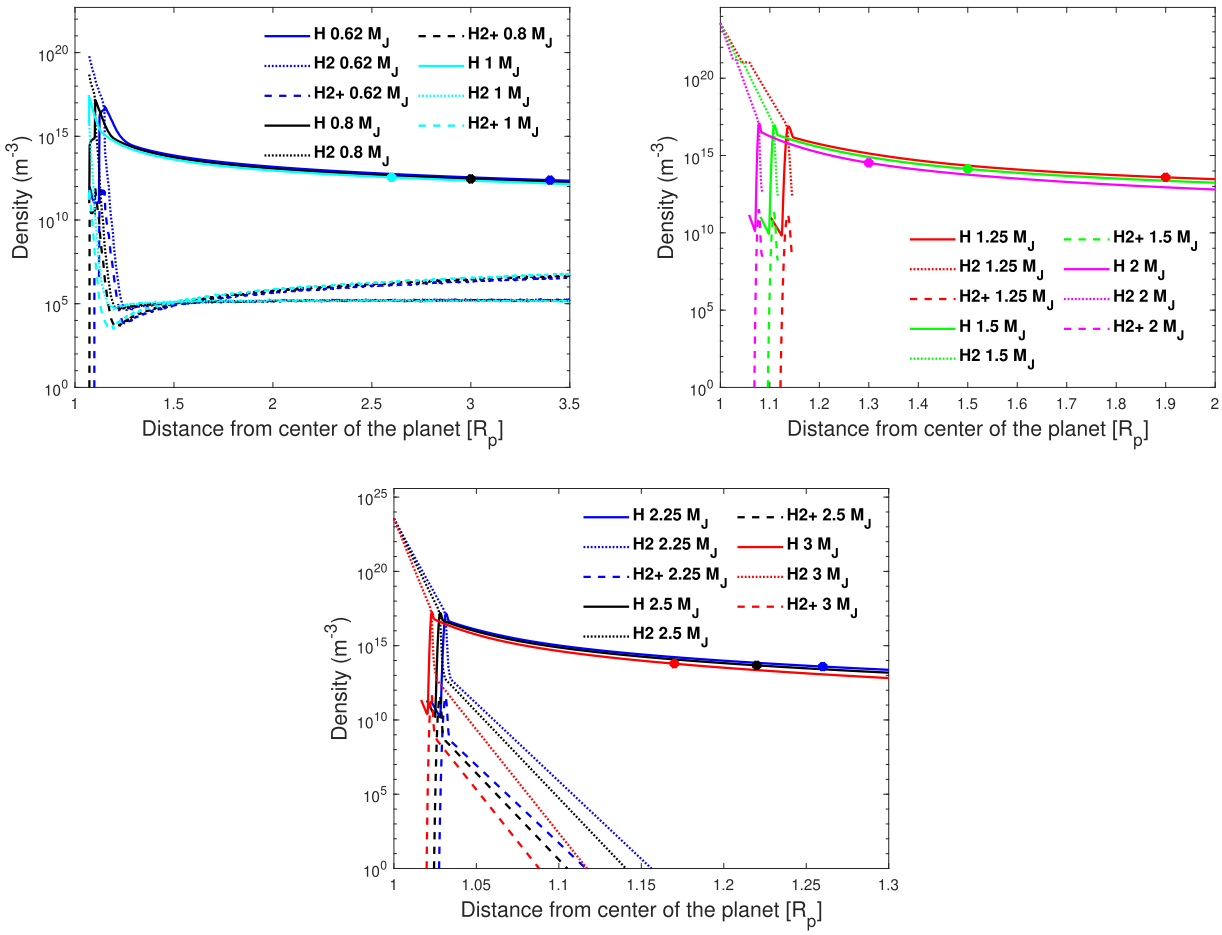

Figure 2. Total H (sum of neutral H and H^+), H_2, and H_2^+ density profiles. First panel: planetary mass cases $M = 0.62$, 0.8, $1.0 M_J$. Second panel: planetary mass cases $M = 1.25$, 1.5, $2.0 M_J$. Third panel: planetary mass cases $M = 2.25$, 2.5, $3.0 M_J$. The dots indicate the corresponding exobase levels.

magnetic moment of $\sim 0.8\,\mathcal{M}_J$, with $\mathcal{M}_J$ the magnetic moment of Jupiter, for the case without tidal locking, with a radio flux of 74 mJy and a maximum emission frequency of 15 MHz. If rotation is important, they find a much lower magnetic moment ($\sim 0.1\,\mathcal{M}_J$) and a maximum emission frequency of 2.5 MHz. In that case, the maximum emission frequency is below Earth's ionospheric cut-off, and the emission would not be detectable with ground-based radio telescopes.

2.3 Planetary atmospheric model

For the atmospheric model, we use the same approach as described in detail in Weber et al. (2018). We apply a 1D time-dependent upper atmosphere model that is described in detail in Erkaev et al. (2016), Kubyshkina et al. (2018a, b, 2019), and Odert et al. (2020). The model solves the system of fluid equations for mass, momentum, and energy conservation in spherical coordinates, includes heating by stellar XUV radiation, Lyman α cooling, ionization and dissociation of hydrogen as well as the relevant hydrogen chemistry.

This model is applied from the planetary surface up to the exobase. For the exobase (marked by a filled circle in Figs 2 to 6), we use the altitude corresponding to a Knudsen number of $Kn = 0.1$. Above the exobase, there is a transition region. In this region (with Knudsen number $0.1 < Kn < 1$), the atmosphere goes from a fluid regime to a purely kinetic situation. In this region, we continue to apply our hydrodynamic/hydrostatic models; this leads, for example, to a continued temperature variation with altitude (see Fig. 3). Above this transition region lies the collisionless region ($Kn > 1$). For this region (which we consider only for planetary masses $\geq 2.25 M_J$), we apply the analytical solution suitable for a collision-free atmosphere (Öpik & Singer 1961); this leads, for example, to a constant temperature value (see Fig. 3). For the region below the exobase, the model converges to a hydrodynamic solution for planetary masses $\leq 1\ M_J$, whereas a hydrostatic solution was found for higher mass cases.

Table 1 lists the parameters that we use for ups And b and its host star. The atmospheric pressure P_0 was chosen so as to obtain an optical depth of unity (for details see Weber et al. 2018), and the atmospheric temperature T_0 was obtained as the equilibrium temperature at the planet's orbit.

An important ingredient in the atmospheric model is the stellar XUV flux (for details see Erkaev et al. 2016; Weber et al. 2018; Kubyshkina et al. 2018a; Odert et al. 2020). The XUV flux is primarily determined by the planet's orbital distance and the stellar age. We use the XUV flux from the study of Sanz-Forcada et al. (2011). For each planetary mass case, we calculate the exobase level, i.e. the altitude above which the atmosphere is no longer dominated by collisions. Table 2 shows that with increasing planetary mass, the exobase level decreases, as a higher gravitational attraction results in a more compact atmosphere. At the same time, a higher mass

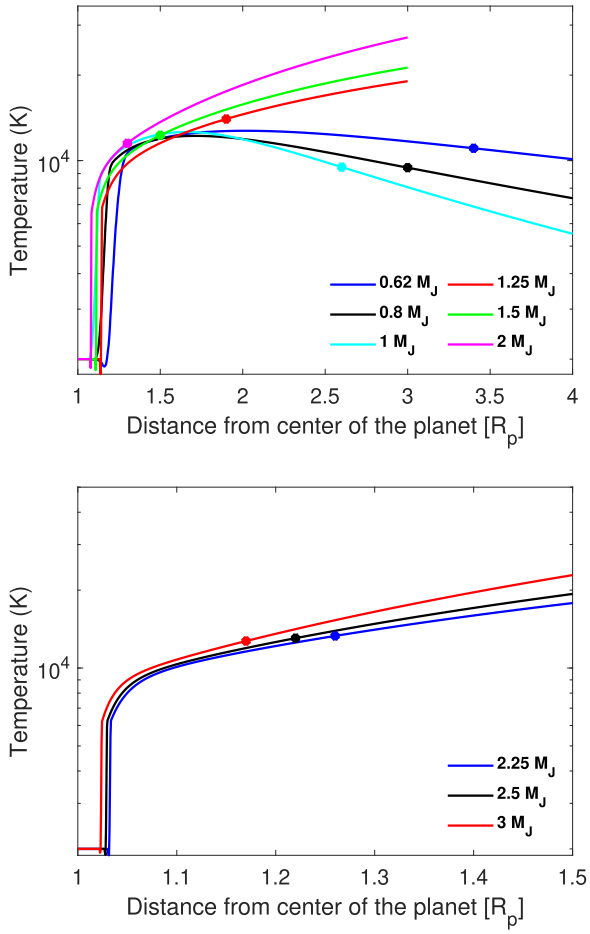

Figure 3. Temperature profiles for the different planetary mass cases. The dots indicate the corresponding exobase levels.

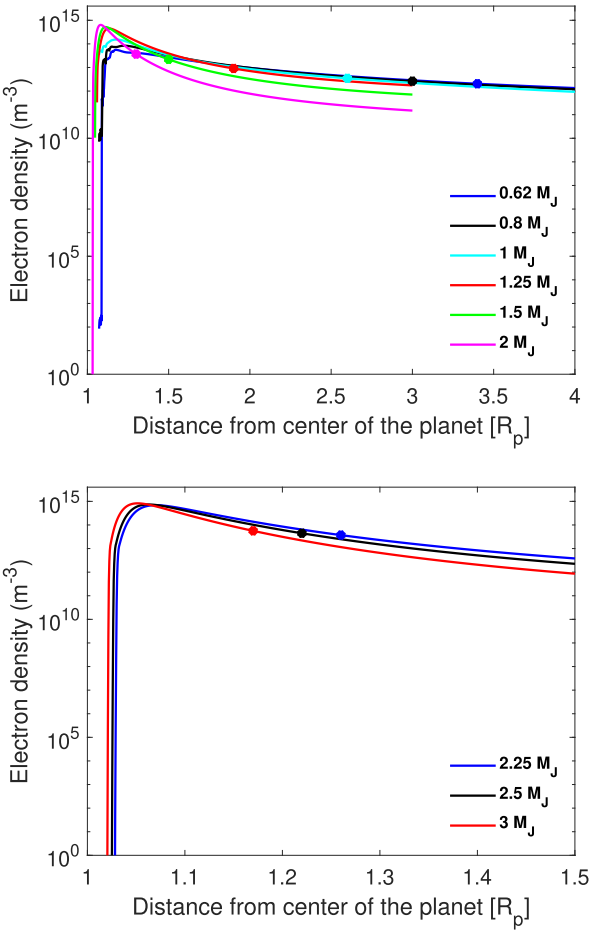

Figure 4. Electron density profiles for the different planetary mass cases. The dots indicate the corresponding exobase levels.

leads to a higher magnetic moment estimate, and thus a higher magnetospheric standoff distance. This is also shown in Fig. 1. The blue line shows the exobase level. The red and green lines indicate the magnetospheric standoff distance with and without influence of tidal locking, respectively (see Section 2.2).

The upper atmosphere model allows us to calculate atmospheric profiles, i.e. number densities of different species as a function of the altitude. Fig. 2 shows the number density profiles of total H (sum of neutral H and H^+), H_2, and H_2^+ (i.e. neutrals and ions) for different planetary masses. The corresponding temperature profiles for different mass cases are shown in Fig. 3. The points on the profiles indicate the corresponding exobase level.

A clear difference can be seen between the cases with extended upper atmosphere and plasma environments ($M \leq 1.0\,M_J$, first panel of Fig. 2) and the cases with a compact atmosphere and compact plasma environments ($M \geq 1.25\,M_J$, second and third panel of Fig. 2). This can also be seen in the temperature profiles (Fig. 3). For the low-mass cases ($M \leq 1.0\,M_J$), the temperature profiles are not monotonic: after reaching a maximum value, the temperature decreases at large distances due to adiabatic cooling in the hydrodynamic flow. For higher masses ($M \geq 1.25\,M_J$), however, the atmospheric profiles are hydrostatic, and no such temperature decrease is observed. For very high masses ($M \geq 2.25\,M_J$), the upper atmosphere is entirely collisionless, and the temperature stays constant.

The resulting electron density profiles for the different planetary mass cases are shown in Fig. 4. Again, dots in colours corresponding to the different mass cases indicate the exobase levels. The electron density profile shows a marked difference between the cases with low to intermediate mass ($M \leq 2.0\,M_J$) and the higher mass cases ($M \geq 2.25\,M_J$). This is due to the fact that for high-mass planets, the exobase and the transition region are much closer. The electron density decreases more rapidly in the collisionless region at high altitudes, leading to lower electron number densities than for lower mass planets.

In the following text, we will check how these different atmospheric structures influence the ratio of plasma and cyclotron frequency. This has important implications for potential planetary radio emission.

3 PLASMA ENVIRONMENT AND CHARACTERISTIC FREQUENCIES

Based on the magnetic and the atmospheric models of Section 2, we evaluate the local electron cyclotron frequency and the local plasma frequency as a function of altitude. This will allow to check whether the condition required for the CMI (i.e. $f_p \ll f_c$) is fulfilled.

For the local cyclotron frequency f_c, we use

$$f_c = \frac{1}{2\pi}\frac{e \cdot B}{m_e}. \quad (1)$$

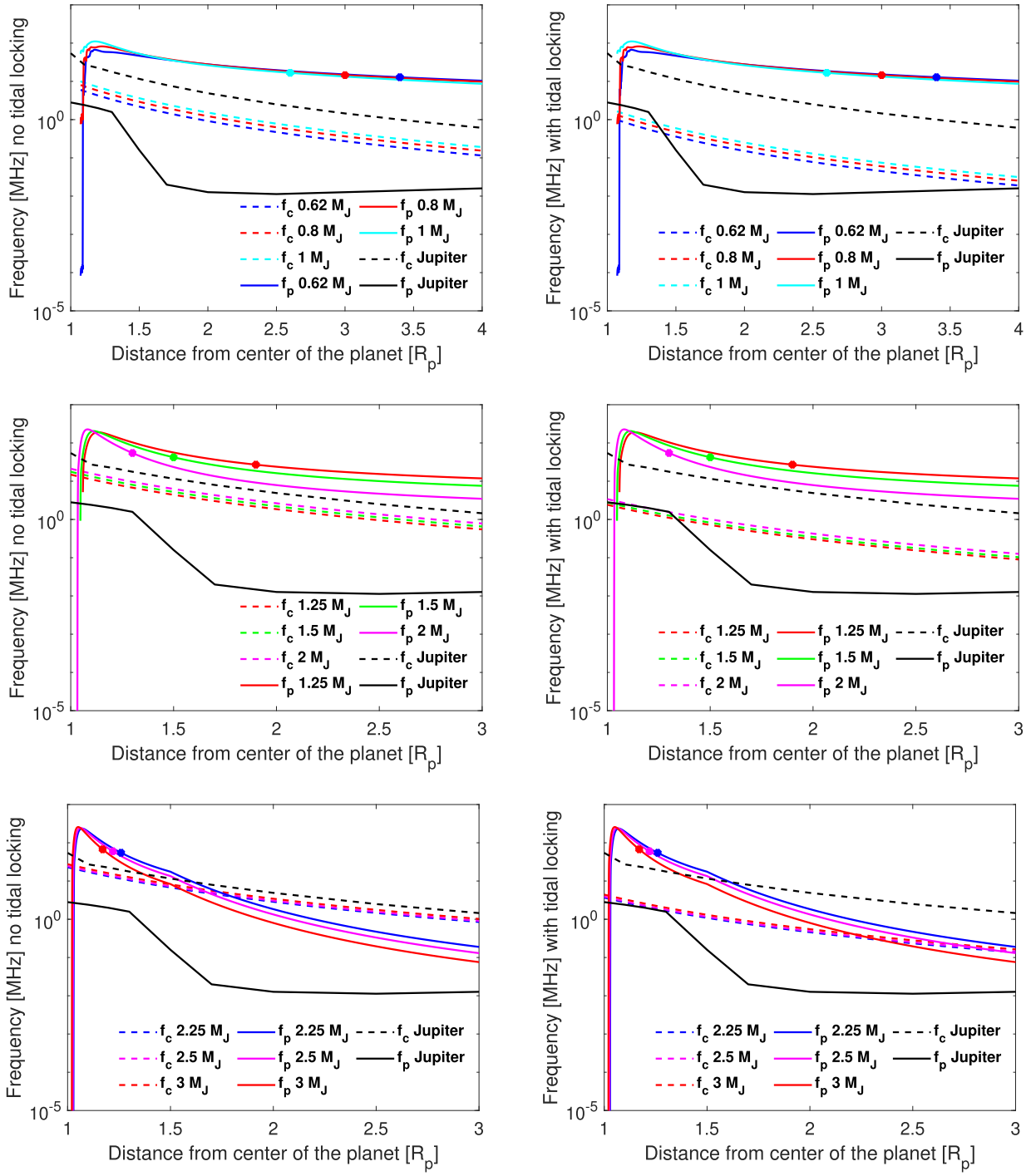

Figure 5. Cyclotron and plasma frequency, considering different magnetic fields for each mass case according to Table 2. Left column: assuming no tidal locking (or a rotation-independent magnetic field); right column: assuming tidal locking. The dots indicate the corresponding exobase levels. In each panel the Jupiter case is shown for comparison.

Here, e is the electron charge, B the local magnetic field strength, and m_e the electron mass. The relation between the magnetic dipole moment $\mathcal{M}$ and the magnetic field strength B above the pole is given by

$$B(r) = \frac{\mu_0}{4\pi}\frac{\mathcal{M}}{r^3}, \tag{2}$$

where $r > R_p$, R_p is the planetary radius, μ_0 is the vacuum permeability, and $\mathcal{M}$ is the planetary magnetic dipole moment.

The local plasma frequency is calculated via

$$f_p = \frac{1}{2\pi}\sqrt{\frac{e^2 n_e}{m_e \varepsilon_0}}, \tag{3}$$

with n_e the local electron density and ε_0 the vacuum permittivity.

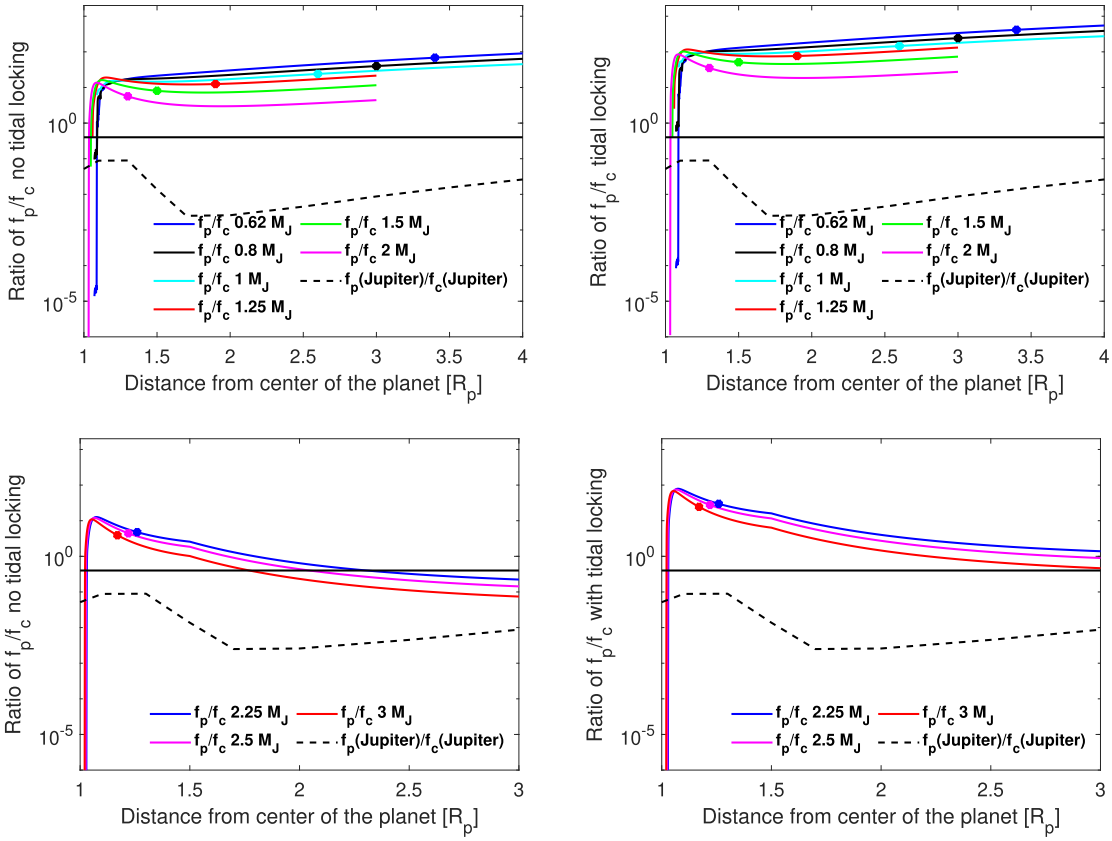

Figure 6. Ratio of plasma to cyclotron frequency, considering different magnetic fields for each mass case according to Table 2. Left column: assuming no tidal locking (or a rotation-independent magnetic field); right column: assuming tidal locking. The dots indicate the corresponding exobase levels. In each panel the Jupiter case is shown for comparison, based on Fig. 5.

Fig. 5 compares the resulting electron cyclotron frequencies to the plasma frequencies. The left-hand panels show cases without influence of tidal locking (or a rotation-independent magnetic moment), the right-hand ones with tidal locking. From top to bottom, the planetary mass increases, and the atmosphere is getting more and more compact. For comparison, each panel also shows the cyclotron and plasma frequency for Jupiter.

In order to facilitate the comparison of the plasma frequency and the cyclotron frequency, one can directly show the ratio between both. Fig. 6 shows this ratio. Again, the left-hand panels show cases without influence of tidal locking (or a rotation-independent magnetic moment), and the right-hand ones with tidal locking. Jupiter is shown for comparison. According to Fig. 6, planetary radio emission is possible (i.e. the frequency ratio is below the critical ratio of 0.4) for ups And b-like planets if the planetary mass is at least 2.25 M_J and there is no tidal locking. If the planetary mass is less or equal than 2 M_J, radio emission is not possible. If tidal locking holds and has an influence on planetary radio emission, no detectable radio emission is expected from ups And b.

4 DISCUSSION

For the parameters of the ups And system as given in Table 1, the upper atmosphere of the studied ups And b cases becomes hydrostatic and hence compact for planetary masses above approximately 1 Jovian mass. For a planetary mass $M \leq 1\ M_J$, the planetary atmosphere is extended, whereas it is compact for a planetary mass $\geq 1.25\ M_J$. The hydrostatic nature of the planet's atmosphere can be seen very well in the density profiles of Fig. 2 (note the different radial axes for the two panels) and in the temperature profiles in Fig. 3. In these cases the exobase level and hence the upper atmosphere remains close to the planetary radius, while the exobase levels for the lower mass cases are located at larger distances. The corresponding temperature profiles in Fig. 3 also show that the lower mass planet cases start to cool adiabatically due to the upward flow of the hydrogen gas, while the heavier planets show a hydrostatic behaviour. Following previous studies (Weber et al. 2017a, b, 2018), we do expect a transition to more favourable conditions for the CMI when the atmosphere becomes compact, i.e. at a planetary mass $\geq 1.25\ M_J$.

The findings presented in Section 3 (Fig. 6) show that this is not sufficient. Indeed, a planetary mass of at least $\geq 2.25\ M_J$ is required for favourable conditions for planetary radio emission. Close inspection of Fig. 5 shows that the cyclotron frequencies are similar for planets above and below 2 M_J. The plasma frequencies, however, differ considerably, with important consequences on detectable radio emission. Only for masses $\geq 2.25\ M_J$ and without tidal locking generation and escape of radio emission is possible in the region up to 3 planetary radii. This confirms that the possibility of planetary radio emission does indeed depend on the compactness of the planetary atmosphere. The critical planetary mass above which the planetary atmosphere becomes 'sufficiently compact' to allow the CMI to operate cannot be determined by simple criteria (such as scaling laws); it can, however, be calculated, as demonstrated.

The argument between planetary mass and the potential for planetary radio emission can also be reversed. If the tentative detection

of radio emission from the planetary system ups And presented by Turner et al. (2021) is confirmed by follow-up observations, and if the planetary origin of the emission is confirmed, it is very likely that the planet has a mass $\geq 2.25\,M_J$, and that its atmosphere is 'compact' (i.e. in hydrostatic state rather than in hydrodynamic state). This value would be compatible, but considerably more constraining, than the lower mass limit of $0.62\,M_J$ obtained from radial velocity measurements. Assuming randomly distributed orbital inclinations, only ∼3 per cent of all radial-velocity-detected planets have a true mass at least four times the projected mass. Due to stability arguments, a random orientation can however not be expected for this system, and a planetary mass of 1–2 M_J seems more likely (McArthur et al. 2010). If a planetary mass of $\geq 2.25\,M_J$ can be attributed to ups And b by future radio observations, this would constitute an interesting finding, and open a new avenue to put much stronger constraints on the masses of extrasolar planets.

5 CONCLUSIONS

Turner et al. (2021) report a tentative detection of radio emission from the system ups And. If this signal is confirmed and its planetary origin can be proven by follow-up observations, this poses strong additional constraints on the planetary mass, for which currently only a minimum value is known from radial velocity measurements. A detected radio signal from this planet would indeed show that the atmosphere is 'compact' (hydrostatic), so that radio waves can be generated and escape from the source region. According to our calculations, radio emission can only be generated at ups And b if the planet has a mass of at least $\geq 2.25\,M_J$ and if tidal locking has no influence. This opens an exciting new avenue to put much stronger constraints on the masses of extrasolar planets.

ACKNOWLEDGEMENTS

This research has used the Extrasolar Planet Encyclopaedia (exoplanet.eu) maintained by J. Schneider (Schneider et al. 2011). C. Weber, H. Lammer, and P. Odert acknowledge support from the FWF project P27256-N27 'Characterizing Stellar and Exoplanetary Environments via Modeling of Lyman-α Transit Observations of Hot Jupiters'. PO acknowledges the Austrian Science Fund (FWF): P30949-N36. NV Erkaev acknowledges support from the Russian Science Foundation project 18-12-00080 in the frame of hydrodynamic/hydrostatic simulation of the planetary upper atmosphere.

DATA AVAILABILITY

The data underlying this article will be shared on reasonable request to the corresponding author.

REFERENCES

Baines E. K., McAlister 1. H. A., ten Brummelaar T. A., Turner N. H., Sturmann J., Sturmann L., Goldfinger P. J., Ridgway S. T., 2008, ApJ, 680, 728
Butler R. P., Marcy G. W., Williams E., Hauser H., Shirts P., 1997, ApJ, 474, L115
Butler R. P., Marcy G. W., Fischer D. A., Brown T. M., Contos A. R., Korzennik S. G., Nisenson P., Noyes R. W., 1999, ApJ, 526, 916
Curiel S., Cantó J., Georgiev L., Chávez C. E., Poveda A., 2011, A&A, 525, A78
Daley-Yates S., Stevens I. R., 2017, Astron. Nachr., 338, 881
Daley-Yates S., Stevens I. R., 2018, MNRAS, 479, 1194
Deitrick R., Barnes R., McArthur B., Quinn T. R., Luger R., Antonsen A., Benedict G. F., 2015, ApJ, 798, 46
Ergun R. E., Carlson C. W., McFadden J. P., Delory G. T., Strangeway R. J., Pritchett P. L., 2000, ApJ, 538, 456
Erkaev N. V., Lammer H., Odert P., Kislyakova K. G., Johnstone C. P., Güdel M., Khodachenko M. L., 2016, MNRAS, 460, 1300
Farrell W. M., Desch M. D., Zarka P., 1999, J. Geophys. Res., 104, 14025
Fuhrmann K., Pfeiffer M. J., Bernkopf J., 1998, A&A, 336, 942
Griessmeier J.-M., 2017, Planetary Radio Emissions VIII, Austrian Academy of Sciences, Graz, Austria, p. 285
Grießmeier J.-M. et al., 2004, A&A, 425, 753
Grießmeier J.-M., Zarka P., Spreeuw H., 2007, A&A, 475, 359
Grießmeier J.-M., Zarka P., Girard J. N., 2011, Radio Sci., 46, RS004752
Hilgers A., 1992, Geophys. Res. Lett., 19, 237
Ito T., Miyama S. M., 2001, ApJ, 552, 372
Kubyshkina D. et al., 2018a, A&A, 619, A151
Kubyshkina D. et al., 2018b, ApJ, 866, L18
Kubyshkina D. et al., 2019, A&A, 632, A65
Le Queau D., Pellat R., Roux A., 1985, Ann. Geophys., 3, 273
Ligi R. et al., 2012, A&A, 545, A5
McArthur B. E., Benedict G. F., Barnes R., Martioli E., Korzennik S., Nelan E., Butler R. P., 2010, ApJ, 715, 1203
Odert P. et al., 2020, A&A, 638, A49
Öpik E. J., Singer S. F., 1961, Phys. Fluids, 4, 221
Reiners A., Christensen U. R., 2010, A&A, 522, A13
Roell T., Neuhäuser R., Seifahrt A., Mugrauer M., 2012, A&A, 542, A92
Ryabov V. B., Zarka P., Ryabov B. P., 2004, Planet. Space Sci., 52, 1479
Sanz-Forcada J., Micela G., Ribas I., Pollock A. M. T., Eiroa C., Velasco A., Solano E., García-Álvarez D., 2011, A&A, 532, A6
Schneider J., Dedieu C., Sidaner P. L., Savalle R., Zolotukhin I., 2011, 532, A79
Shiratori Y., Yokoo H., Saso T., Kameya O., Iwadate K., Asari K., 2006, in Arnold L., Bouchy F., Moutou C., eds, Tenth Anniversary of 51 Peg-b: Status of and Prospects for Hot Jupiter Studies. Observatoire de Haute Provence, p.France, 290
Treumann R. A., 2006, A&AR, 13, 229
Turner J. D. et al., 2021, A&A, 645, A59
Weber C. et al., 2017a, in Fischer G., Mann G., Panchenko M., Zarka P., eds, Planetary Radio Emissions VIII. Austrian Academy of Sciences Press, Vienna, p. 317
Weber C. et al., 2017b, MNRAS, 469, 3505
Weber C., Erkaev N. V., Ivanov V. A., Odert P., Grießmeier J.-M., Fossati L., Lammer H., Rucker H. O., 2018, MNRAS, 480, 3680
Winterhalter D. et al., 2006, in Rucker H. O., Kurth W., Mann G., eds, Planetary Radio Emissions VI. Austrian Academy of Sciences, Graz, Austria, p. 595
Zarka P., 1998, J. Geophys. Res., 103, 20159
Zarka P., Queinnec J., Crary F. J., 2001, Planet. Space Sci., 49, 1137

This paper has been typeset from a TEX/LATEX file prepared by the author.